Hindawi Publishing Corporation
Journal of Solid State Physics
Volume 2015, Article ID 549314, 6 pages
http://dx.doi.org/10.1155/2015/549314

Research Article

Recrystallization from a Three-Grain Crystalline Iron

Bo Zhao,[1,2] Shanshan Chen,[1,2] Jinfan Huang,[2] and Lawrence S. Bartell[2]

[1]*Department of Chemistry, Nanjing Normal University, Nanjing, China*
[2]*Department of Chemistry, University of Michigan, 930 N. University Avenue, Ann Arbor, MI 48109, USA*

Correspondence should be addressed to Jinfan Huang; jinfanh@umich.edu

Received 30 August 2014; Revised 27 December 2014; Accepted 28 December 2014

Academic Editor: Víctor Lavín

The solid state recrystallization and grain boundary migrations in an iron nanoparticle Fe_{2616} with three grains were studied by a molecular dynamics simulation. It was found that nucleation rates could be determined as the smaller grains were consumed by the larger ones. Moreover, the grain disorder was more important than the misorientation angle in governing the rates. Suggestions about the critical nuclei for the recrystallization are proposed. No obvious interaction between the grain boundaries was observed in the example studied in this report.

1. Introduction

Recrystallization is the formation of a new grain structure in a solid material by the migration of grain boundaries that results in larger grains. This spontaneous process is considered to be driven by the excess energy in grain boundaries [1] but we have found that grain disorder is also important. Most industrial metals contain numerous grains and the new grain structure forms when larger grains grow by consuming the smaller adjacent ones. Understanding of the details of the solid state recrystallization behavior of metals and semiconductors in the thermomechanical or annealing processes is of importance because it can have a strong influence on the microstructure and texture of solids. From an understanding of this, a metallurgist is able to control the microstructure of metals and therefore improve the properties during thermomechanical processing. And material scientists may be able to control the crystal growth in the semiconductor industries once they understand the principles of recrystallization. However, several aspects of recrystallization, such as the almost universally proposed nucleation and grain boundary migration, are poorly understood at the atomic level [1–3]. Consequently computer molecular dynamics (MD) simulations provide an alternative and promising approach to study aspects of solid state recrystallization. Because none of the crystalline grains in this MD study are completely surrounded by other grains in the simulations, the behavior is not directly analogous to the behavior of grains in bulk studies but it is an initial step in understanding what happens when small grains are consumed by larger ones.

In the past decade, we have used the MD technique to study nucleation in the crystallization of molten materials and in phase transitions between different solid phases of nanometer size. To explore recrystallization in solids, we began an MD study on the simplest system, an iron nanoparticle Fe_{1436} with only two grains, and observed the thermal annealing process [4]. We found that the rate of transformation is not necessarily determined by the degree of misorientation between the grains, as seems to be the case in bulk experiments. Instead, the degree of the disorder of the starting grains plays a more important role. Although the interfacial migration does not differ from that in the earlier study, the dependence on grain size and relative stability of the grains can be observed. We are approaching the problem of solid state recrystallization in stages of complexity in order to better interpret the atomic activity involved. In this paper we report the MD simulation results on an iron nanoparticle, Fe_{2616}, which included three grains with a larger grain in the middle and sandwiched by two smaller grains.

2. Computational Procedures

2.1. Generation of Polycrystalline Nanoparticles for Recrystallization Study. Molecular dynamics simulations were performed on a solid state polycrystalline iron nanoparticle

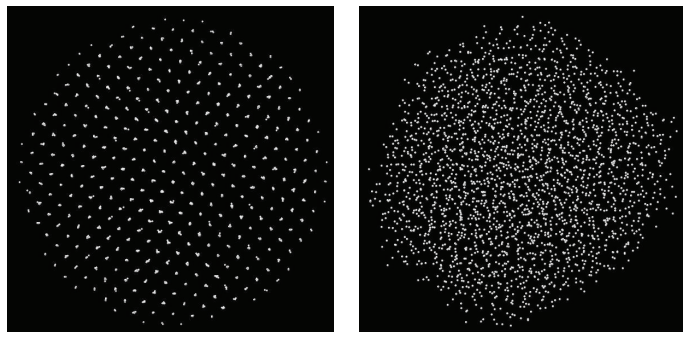

(a) Starting point

(b) Molten droplet at 1680 K

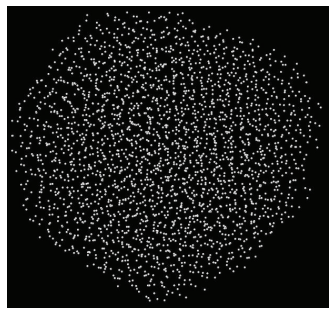

(c) One of 18 molten particles with different thermal history

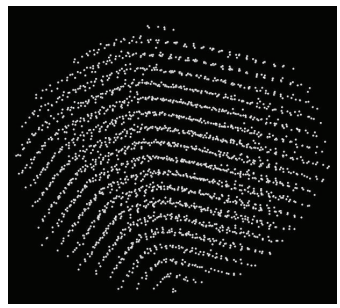

(d) Polycrystal after quenching to 850 K

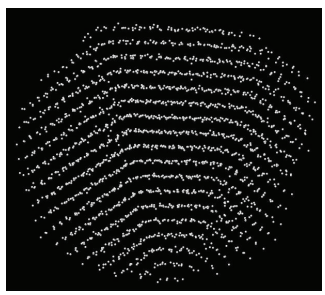

(e) Polycrystal after quenching to 850 K

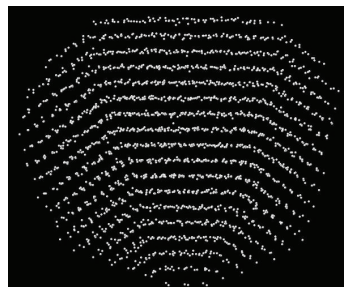

(f) Polycrystal after quenching to 850 K

Figure 1: Images of the nanoparticles from various processing stages and different quenching runs.

Fe_{2616}. The program XMD [5] was employed to carry out the simulation with an embedded-atom method (EAM) potential [6, 7] and 2 fs time step was used in all of the simulations.

The studied quasispherical iron particle containing 2616 iron atoms was first cut from a body-center cubic (BCC) lattice of iron (Figure 1(a)). The MD simulations began at constant temperature with 50,000 time steps in a bath at 200 K. A series of heating stages started at 300 K with increments of 20 K; each stage was run at constant temperature for 50,000 time steps. The Fe_{2616} nanoparticle was heated to 1680 K to obtain a completely melted nanodroplet (Figure 1(b)). The molten nanodroplet was then cooled to 1660 K and simulations were continued to form 18 Fe_{2616} nanodroplets with different thermal histories, each with 50,000 more time steps than the previous one.

One image of molten particles is given in Figure 1(c). These 18 melted Fe_{2616} nanodroplets were quenched into heat bath at a temperature of 850 K, and all of them froze into polycrystalline nanoparticles. Figures 1(d), 1(e), and 1(f) show the images of three of them. The nanoparticle with three grains as depicted in Figure 1(f) was selected for the recrystallization.

To observe the stochastic behavior of the recrystallization, it is necessary to generate ensembles of systems with different thermal histories. Therefore the selected three-grain polycrystalline particle shown in Figure 1(f) was then heated at 900 K, to generate 18 particles, each particle experiencing 2000 more time steps than the previous one. These 18 particles were then annealed at constant temperature in a heat bath of 850 K. The simulation time length for each member of the ensemble at this stage was determined by the formation of the final single crystalline solid.

2.2. Analysis of the Recrystallization Process. Recrystallization is said to be initiated by nucleation. What is observed to happen is that the crystalline planes of the smaller grains

become disrupted, making the grain appear to become amorphous. Then some stochastic, first-order process begins to form crystalline planes coincident with those of the larger, adjacent crystal. While this process has some of the earmarks of nucleation, regrettably we so far lack an adequate knowledge of the characteristics defining nuclei for recrystallization.

The recrystallization of grain structure is accompanied by energy changes. Therefore a transition in a given particle can be recognized by a sudden change in the slope of energy as a function of temperature during an annealing run. Monitoring structural changes is an effective alternative analysis method to energy, during freezing and recrystallization. Structural changes were followed by observing the linearity in the arrays of atoms corresponding to BCC cell edges. Deviations from linearity disclosed dislocations.

For an ideal BCC lattice, each atom and its nearest 8 coordination atoms, the corner atoms, form a body-centered cubic unit cell. Each atom in an array along cell edges is located at the crossing point of three orthogonal axes that connect the corners of the cells. Taking this crossing of central atoms as an origin, at the ends of the three orthogonal cell edges are 6 atoms appearing as sharp spots for a perfect crystal. For the sake of simplicity, we only consider the lines connecting an array of three atoms, with the central atom at the corner of a BCC cell, which is shared by BCC cells in the bulk case. For imperfectly packed nanoparticles these six spots may be diffuse.

Line of three atoms along a cell edge may be far from linear because of a surface or other imperfections, and if there are fewer than three nearly orthogonal lines crossing a cell corner, we will refer to these cases as having fewer than three "cross-overs" and use these in an analysis of dislocations and surfaces. In determining the number of "cross-overs" we considered neighboring atoms within the range of 2.76–2.96 Å lying along directions within 4° of perfect orthogonality [4].

2.3. Estimation of Recrystallization Rate. Inasmuch as the recrystallization rate was observed to evolve into a first-order process, it is possible to interpret results in terms of classical nucleation theory as follows. The fraction of particles, in which a postulated nucleation site for recrystallization has not yet formed, obeys the first-order rate law

$$\ln \frac{N_n(t)}{N_0} = -JV_c\left(t_n - t_0\right), \tag{1}$$

where N_0 is the total number of particles in the assembly, V_c is the effective volume for the proposed nucleation, and J is the nucleation rate, t_n is the time at which the nth transition in the set of N_0 particles has taken place, t_0 is the time lag to achieve a steady state of precritical nuclei, and $N_n(t)$ is defined as

$$N_n(t) = N_0 - n + 1. \tag{2}$$

From the slope of the curve $\ln[N_n(t)/N_0]$ versus $(t_n - t_0)$, J, the rate of recrystallization, can be obtained. The times t_n in the ensemble are estimated from the sudden changes in the energy-time curves of members of the ensemble. We take V_c to be the volume of the layer with three-atom thick grain boundary at the interface of the grain that is transforming. To account for the appreciable statistical uncertainties associated with the stochastic nature of the hypothetical nucleation events when N_0 is small, a weighted least-squares procedure was carried out to determine J and t_0. Details are given in our previous report [8].

3. Results

3.1. Grain Boundary Migration and Grain Growth. Figure 2 displays images of a nanoparticle at various times during the annealing run from one of the 18 particles with different thermal histories. Laboratory experiments indicate that recrystallization proceeds first from the migration of high angle grain boundaries away from a more crystalline matrix. Whether this is true for simulations is considered in the following. Migration is driven by the energy gradient across the boundary between grains. For the displayed nanoparticle the conspicuous change began when the particle had been annealed for about 322 ps from the beginning. The image changed quickly after 322 ps and the entire reorganization ended within 34 ps while the smallest grain on the right side was completely transformed as shown in Figure 2(e). The grain boundary motion can be seen in the three snapshots of such moving given in Figures 2(b), 2(c), and 2(d).

As seen in Figure 2, the left grain boundary remains unchanged even after the right boundary has completely disappeared (Figures 2(a)–2(e)). The recrystallization along this boundary started at 528 ps (Figure 2(f)), about 162 ps after the completion of the recrystallization of the right-hand grain. The grain growth and the grain boundary migration speed along this grain boundary were faster, and the particle finally became a single crystal within 28 ps. The time range for the recrystallization and the grain growth is between 322 ps and 356 ps near the right grain boundary, while it is between 528 ps and 556 ps along the left side boundary.

3.2. Strain Energy and Initiation of Recrystallization. Figure 3 plots the total energy as a function of time that the molten droplet spent in the 850 K heat bath from the quenching run that formed the tricrystalline particle shown in Figure 1(f). From Figure 3 it can be seen that when the molten droplet was quenched into the heat bath of 850 K the total energy dropped very sharply around 7700 ps (this time including all the heating history for the particle started at 200 K) due to the sudden temperature change that produced a supercooled liquid droplet (Figure 1(c)). The first sudden energy change of the droplet at about 8000 ps in the curve corresponds to the freezing of the liquid droplet into a polycrystalline solid (Figure 1(d)). The second sharp energy change indicates a recrystallization process from the polycrystalline particle transforming from the droplet into a particle with three grains (Figure 1(e)).

Figure 4 gives the total energy change at higher resolution than in Figure 3 from the annealing at 850 K for the tricrystalline particle selected (Figure 2(a)). Two sharp energy drops are seen. The first one began when the nanoparticle was

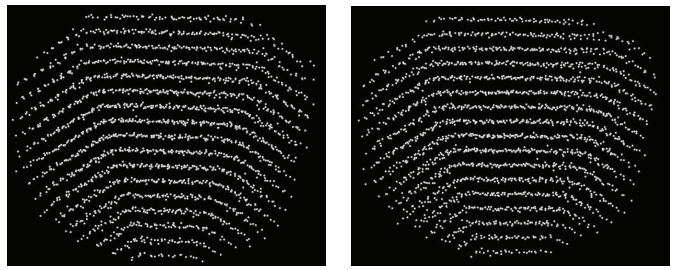

(a) (Begin) (b) (220 ps)

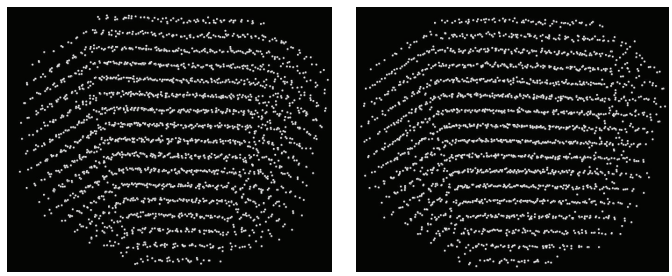

(c) (322 ps) (d) (336 ps)

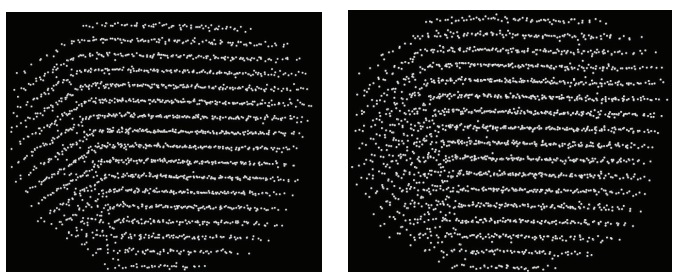

(e) (356 ps) (f) (528 s)

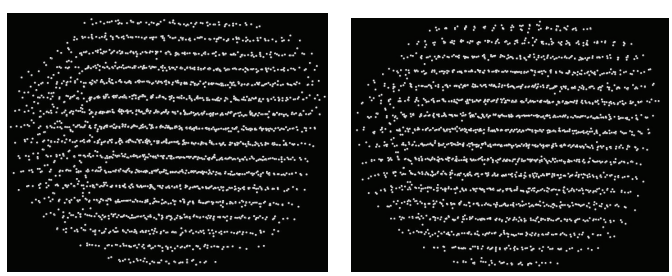

(g) (536 ps) (h) (538 ps)

(i) (556 ps) (j) (872 ps)

Figure 2: Images of nanoparticle at various times during the annealing run.

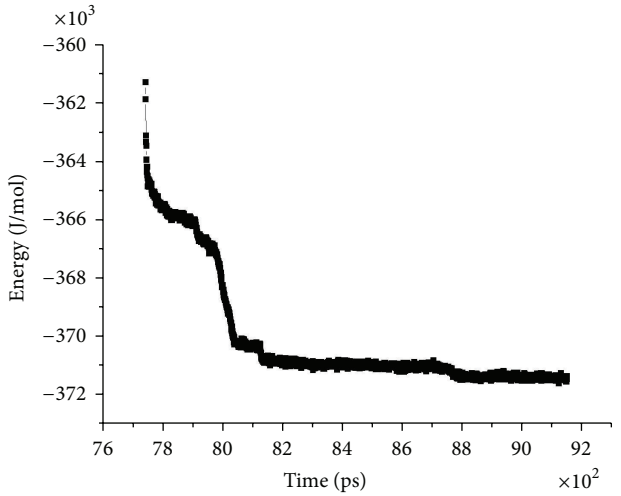

FIGURE 3: The total energy as a function of time during the quenching run at 850 K in unit of J/mol.

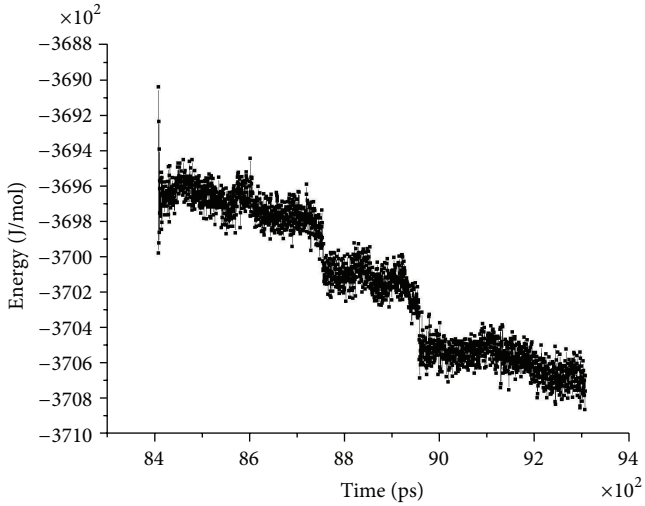

FIGURE 4: The total energy as a function of time during the annealing run in unit of J/mol.

annealed for about 322 ps (8722 ps on the curve), consistent with the beginning of the transformation of the right grain shown in Figure 2(c). The second transition began at about 536 ps (8936 ps on the curve) after annealing, a time agreeing well with the transformation of the left grain (Figure 2(f)).

The time between when the tricrystalline particle was put into the heat bath of 850 K and the onset of the first sharp energy drop from Figure 4 can be considered as the presumed nucleation time for the recrystallization of the right grain. It is shorter than the time for the left-hand grain. The time of nucleation applicable to nucleation theory is t_0, the time at which $\ln[N/N_o]$ is zero.

3.3. Rates of the Recrystallizations. Figure 5 shows the plots of $\ln[N_n(t_n)/N_0]$ beginning at t_0 of (1) for each of the grain boundaries. Curve (A) is based on the presumed nucleation events along the right grain boundary and the times of

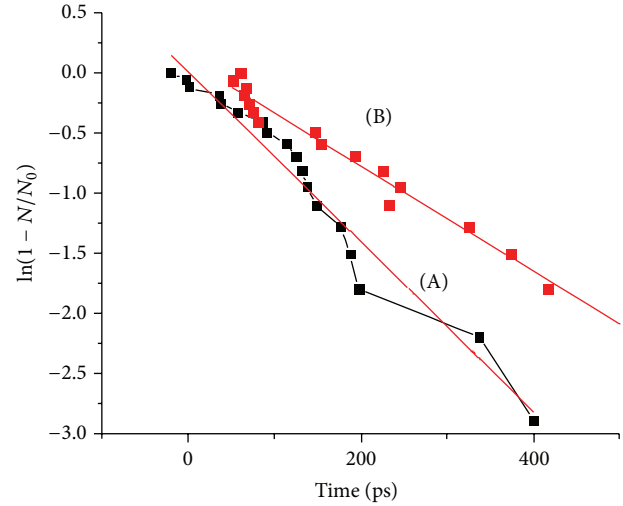

FIGURE 5: $\ln[N_n(t)/N_0] \sim t$ plot for Fe_{2616}. (A) is from nucleation events near the right grain boundary in (A); (B) is from nucleation events near the boundary of the larger left grain.

transition are inferred for each of the 18 particles with independent histories by the onset of their first sharp energy drop. The nucleation rate estimated from the slope of this plot is 2.2×10^{36} m^{-3} s^{-1} if the volume of the grain boundary (assumed to be a layer three atoms thick) is taken as the effective nucleation volume. Curve (B) is from the transition events along the left side grain boundary and the times are inferred as described for curve (A). The nucleation rate at the left boundary is estimated to be 1.5×10^{36} m^{-3} s^{-1} when the volume of the three layers of the grain boundary was used.

4. Discussion

4.1. Recrystallization: Experiments versus MD Simulations. Most of the experimental work in recrystallization research described in the literature begins with a plastically deformed phase, followed by the processes of recovery, recrystallization, and grain growth. At present there is an incomplete understanding of the various rates encountered between deformation and the processes of recovery and recrystallization. This complicates the development of quantitative models of recrystallization. On the other hand, there is a great deal of information about the formation of boundaries during deformation, but theories of annealing are limited. In MD simulations there is no deformation stage because the metal particles are directly annealed from the state in which they were generated. This eliminated certain complications encountered experimentally, allowing us to concentrate on the steps after recovery. The greatest advantage of MD simulation is that the structure changes can be seen at the atomic level and followed during the grain migration.

4.2. The Relationship between Grain Boundary Angles and Transformation Rate. A grain boundary is formed where two single-crystal grains in a polycrystalline aggregate meet and is characterized by five degrees of freedom; these include the

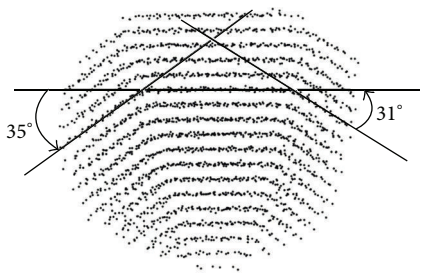

Figure 6: Grain boundary misorientation angles of an Fe_{2616} particle at the beginning of an annealing run.

misorientation of the grains on either side of the boundary (two degrees of freedom for the axis of misorientation and one for the misorientation angle) and the plane of the interface (two degrees of freedom). Once the boundary plane and the rotation axis are determined, then the smallest rotation angle around the rotation axis can be used for the misorientation between two crystal grains. Conventionally, grain boundaries are often grouped into low angle and high angle with the delimiting angle separating low from high angle boundaries of 15°.

Our selected sample was annealed at constant temperature in a bath at 850 K, and recrystallization events were analyzed at the atomic level. Figure 6 shows the grain boundary misorientation angles in our Fe_{2616} particle at the beginning of an annealing run, viewed from a direction almost parallel to the angle bisector of $(0\,\bar{1}\,0)$ and $(00\,\bar{1})$ surfaces of a BCC lattice of the particle. There were three grains in the iron particle with high angle boundaries, which were formed where two single-crystal grains in this aggregate met. It is commonly believed that these boundaries are the major sources of the extra strain energy for recrystallization but our simulations show that the disorders (energy per atom) are important contributors. The right subgrain was the smallest and most disordered.

The recrystallization rates for these two different grains were different. One interesting thing is that the transformation rate for the right grain is higher despite its smaller grain boundary misorientation angle. The factor discriminating between the two rates can be attributed to the greater disorder in the smaller particle despite its lower misorientation angle.

As mentioned before, once a grain boundary starts to move, the time to complete the consumption of the left grain is less than the time used for the right grain despite the slower rate. This counterintuitive effect seems to stem from the fact that, for reasons unknown, the smaller grain takes a longer time in its transformation to develop into first-order kinetics.

4.3. Conjectures about Critical Nuclei in Recrystallization. Presumably any critical nucleus is in the disordered grain and is immediately adjacent to the grain boundary. It must contain atoms in planes with the orientation of the larger grain. Such a nucleus was not conspicuous in our simulation and, regrettably, such a nucleus was not intensively searched for, so it remains speculative.

5. Concluding Remarks

The solid state recrystallization and grain boundary migrations in an iron nanoparticle Fe_{2616} with three grains were studied by a molecular dynamics simulation. Rates were not inconsistent with what would be expected for a process of nucleation though no direct evidence of nuclei was observed. It was found that first-order transformation rates could be determined as the smaller grains were consumed by the larger one. In comparing subgrains, the conclusion that grain disorder was more important than the misorientation angle in governing the rates was reconfirmed in this study. Suggestions about the critical nuclei for the recrystallization are proposed. No obvious interactions between the subsidiary grains boundaries were observed in the example studied in this report.

Conflict of Interests

The authors declare that there is no conflict of interests regarding the publication of this paper.

Acknowledgment

This work was supported in part by the Social Security Administration.

References

[1] R. D. Doherty, D. A. Hughes, F. J. Humphreys et al., "Current issues in recrystallization: a review," *Materials Science and Engineering A*, vol. 238, no. 2, pp. 219–274, 1997.

[2] F. J. Humphreys and M. Hatherly, *Recrystallization and Related Annealing Phenomena*, Elsevier, Oxford, UK, 2nd edition, 2004.

[3] B. Hutchnson, *Thermomechenical Processing in Theory, Modeling and Practice*, ASM International, Material Park, Ohio, USA, 1997.

[4] J. Huang and L. S. Bartell, "Molecular dynamics simulations of solid state recrystallization I: observation of grain growth in annealed iron nanoparticles," *Journal of Solid State Chemistry*, vol. 185, pp. 238–244, 2012.

[5] J. Rifkin, "XMD program," jon.rifkin@uconn.edu at the University of Connecticut.

[6] M. S. Daw, S. M. Foiles, and M. I. Baskes, "The embedded-atom method: a review of theory and applications," *Materials Science Reports*, vol. 9, no. 7-8, pp. 251–310, 1993.

[7] D. Farkas, "Potential data for iron," http://www.ims.uccon.edu/centers/simul/pot/fefarkas.pot.

[8] L. S. Bartell, "Analyses of nucleation rates from molecular dynamics simulations," *Journal of Physical Chemistry A*, vol. 106, no. 45, pp. 10893–10897, 2002.